

Gribov inelastic shadowing in the dipole representation*

B. Z. Kopeliovich

*Departamento de Física, Universidad Técnica Federico Santa María; and
Centro Científico-Tecnológico de Valparaíso; Casilla 110-V, Valparaíso, Chile*

Abstract

The dipole phenomenology, which has been quite successful applied to various hard reactions, especially on nuclear targets, is applied for calculation of Gribov inelastic shadowing. This approach does not include ad hoc procedures, which are unavoidable in calculations done in hadronic representation. Several examples of Gribov corrections evaluated within the dipole description are presented.

* To be published in "Gribov-85 Memorial Volume", World Scientific, 2016.

I. INTRODUCTION

The Glauber model [1] was the first theoretical approach which calculated the effects of shadowing in hadron-nucleus interactions. The model however, was essentially non-relativistic. In the pioneering papers by V.N. Gribov [2, 3] it was realised that the length scales of interaction rising with energy significantly change the pattern of hadron-nucleus interaction at high energies. In particular, particles created in an inelastic collision with one nucleon, can be subsequently absorbed by another bound nucleons. Such corrections make the nuclear medium more transparent for hadrons, and consequently lead to a reduction of the total hadron-nucleus cross section. These corrections, called Gribov inelastic shadowing, improve the Glauber model, making it well-founded.

II. FROM THE GLAUBER MODEL TO THE GRIBOV-GLAUBER THEORY

The amplitude of probability for a hadron to interact with the nucleus is one minus the probability amplitude of no interaction with any of the bound nucleons. So the hA elastic amplitude at impact parameter b has the eikonal form,

$$\Gamma^{hA}(\vec{b}; \{\vec{s}_j, z_j\}) = 1 - \prod_{k=1}^A \left[1 - \Gamma^{hN}(\vec{b} - \vec{s}_k) \right] , \quad (1)$$

where $\{\vec{s}_j, z_j\}$ denote the coordinates of the target nucleon N_j . $i\Gamma^{hN}$ is the elastic scattering amplitude on a nucleon normalized as,

$$\begin{aligned} \sigma_{tot}^{hN} &= 2 \int d^2b \operatorname{Re} \Gamma^{hN}(b); \\ \sigma_{el}^{hN} &= \int d^2b |\Gamma^{hN}(b)|^2 . \end{aligned} \quad (2)$$

In the approximation of single particle nuclear density one can calculate a matrix element between the nuclear ground states.

$$\langle 0 | \Gamma^{hA}(\vec{b}; \{\vec{s}_j, z_j\}) | 0 \rangle = 1 - \left[1 - \frac{1}{A} \int d^2s \Gamma^{hN}(s) \int_{-\infty}^{\infty} dz \rho_A(\vec{b} - \vec{s}, z) \right]^A , \quad (3)$$

where

$$\rho_A(\vec{b}_1, z_1) = \int \prod_{i=2}^A d^3r_i |\Psi_A(\{\vec{r}_j\})|^2 , \quad (4)$$

is the nuclear single particle density.

Eq. (3) is related via unitarity to the total hA cross section,

$$\begin{aligned} \sigma_{tot}^{hA} &= 2 \operatorname{Re} \int d^2b \left\{ 1 - \left[1 - \frac{1}{A} \int d^2s \Gamma^{hN}(s) T_A(\vec{b} - \vec{s}) \right]^A \right\} \\ &\approx 2 \int d^2b \left\{ 1 - \exp \left[-\frac{1}{2} \sigma_{tot}^{hN} (1 - i\rho_{pp}) T_A^h(b) \right] \right\} , \end{aligned} \quad (5)$$

where ρ_{pp} is the ratio of the real to imaginary parts of the forward pp elastic amplitude;

$$T_A^h(b) = \frac{2}{\sigma_{tot}^{hN}} \int d^2s \operatorname{Re} \Gamma^{hN}(s) T_A(\vec{b} - \vec{s}) ; \quad (6)$$

and

$$T_A(b) = \int_{-\infty}^{\infty} dz \rho_A(b, z) , \quad (7)$$

is the nuclear thickness function. We use Gaussian form of $\Gamma^{hN}(s)$ in what follows,

$$\operatorname{Re} \Gamma^{hN}(s) = \frac{\sigma_{tot}^{hN}}{4\pi B_{hN}} \exp\left(\frac{-s^2}{2B_{hN}}\right) , \quad (8)$$

where B_{hN} is the slope of the differential hN elastic cross section. Notice that the accuracy of the optical approximation (the second line in (5)) is quite high for heavy nuclei. For the sake of simplicity, we use the optical form throughout the paper although for numerical evaluations always rely on the accurate expression (the first line in (5)). The effective nuclear thickness, Eq. (6) implicitly contains energy dependence, which is extremely weak.

In what follows we also neglect the real part of the elastic amplitude, unless specified, since it gives a vanishing correction $\sim \rho_{pp}^2/A^{2/3}$.

Besides the total cross section Eq. (5) one can calculate within the Glauber model also elastic, quasielastic (break-up of the nucleus without particle production) and inelastic cross section. One can find details of such calculations, as well as numerical results, in Ref.[4–6], and below in Sect. III B.

The Glauber model is intensively used nowadays as a theoretical tool to study heavy ion collisions. However, this model is subject to significant Gribov corrections [2].

1. Intermediate state diffractive excitations

The Glauber model is a single-channel approximation, therefore it misses the possibility of diffractive excitation of the projectile in the intermediate state as is illustrated in Fig. 1.

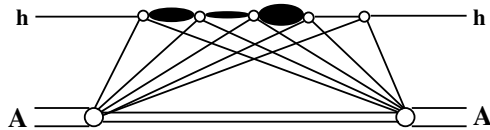


FIG. 1: Diagonal and off-diagonal diffractive multiple excitations of the projectile hadron in intermediate state

Inclusion of multiple diffractive transitions between different excitations, like depicted in Fig. 1, obviously is a challenge, because diffractive transitions between different excited states cannot be measured in diffractive processes. There is, however, one case free of these problems, shadowing in hadron-deuteron interactions. In this case no interaction in the intermediate state is possible, and knowledge of diffractive cross section $hN \rightarrow XN$ is sufficient for calculations of the inelastic correction with no further assumptions. In this

case the Gribov correction to the Glauber model for the total cross section has the simple form [2],

$$\Delta\sigma_{tot}^{hd} = -2 \int dM^2 \int dp_T^2 \frac{d\sigma_{sd}^{hN}}{dM^2 dp_T^2} F_d(4t). \quad (9)$$

Here $F(t)$ is the deuteron electromagnetic formfactor; σ_{sd}^{hN} is the cross section of single diffractive dissociation $hN \rightarrow XN$ with longitudinal momentum transfer

$$q_L = \frac{M^2 - m_h^2}{2E_h}; \quad (10)$$

and $t = -p_T^2 - q_L^2$.

The formula for the lowest order inelastic corrections to the total hadron-nucleus cross section was suggested in [7],

$$\begin{aligned} \Delta\sigma_{tot}^{hA} = & -8\pi \int d^2b e^{-\frac{1}{2}\sigma_{tot}^{hN} T_A(b)} \int_{M_{min}^2} dM^2 \frac{d\sigma_{sd}^{hN}}{dM^2 dp_T^2} \Big|_{p_T=0} \\ & \times \int_{-\infty}^{\infty} dz_1 \rho_A(b, z_1) \int_{z_1}^{\infty} dz_2 \rho_A(b, z_2) e^{iq_L(z_2-z_1)}, \end{aligned} \quad (11)$$

This correction takes care of the onset of inelastic shadowing via phase shifts controlled by q_L and does a good job describing data at low energies [8, 9], as one can also see in Fig. 2.

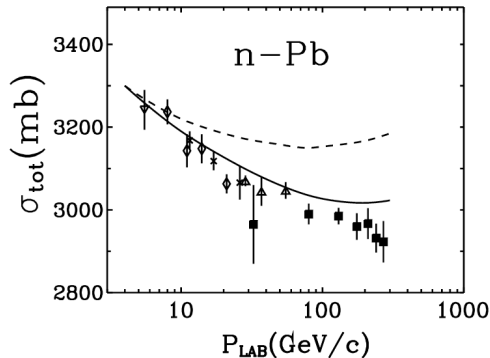


FIG. 2: Data and calculations [8] for the total neutron-lead cross section. The dashed and solid curves correspond to the Glauber model and corrected for Gribov shadowing respectively.

In a similar way Gribov corrections can be calculated for neutrino-nucleus cross section at low Q^2 , when PCAC hypothesis is at work. Then one can employ the Adler relation, which connects neutrino and pion induced cross sections at $Q^2 = 0$, and write the nucleus-to-proton

ration of total neutrino-nucleus cross sections as [10],

$$R_{A/N}^\nu = 1 - \frac{8\pi}{A\sigma_{tot}^{\nu N}} \left. \frac{d\sigma_{diff}^{\nu \rightarrow \pi}}{dp_T^2} \right|_{p_T=0} \int d^2b \int_{-\infty}^{\infty} dz_1 \rho_A(b, z_1) \times \int_{-\infty}^{z_1} dz_2 \rho_A(b, z_2) e^{-iq_L^\pi(z_2-z_1)} e^{-\frac{1}{2}\sigma_{tot}^{\pi N} T_A(b, z_2, z_1)}, \quad (12)$$

where $q_L^\pi = (Q^2 + m_\pi^2)/2\nu$.

At very low energy where q_L^π is large, the second term in (12) is suppressed, and the first one, corresponding to the cross section proportional to A , dominates. At high energies $q_L^\pi \ll R_A$ can be neglected and the integrations over $z_{1,2}$ can be performed analytically [10]. Due to the Adler relation the first term in (12) and the volume part of the second term cancel, and the rest is the "surface" term $\propto A^{2/3}$,

$$\left. \frac{d^2\sigma(\nu A \rightarrow l X)}{dQ^2 d\nu} \right|_{q_L \ll 1/R_A} = \frac{G^2}{2\pi^2} f_\pi^2 \frac{E - \nu}{E\nu} \sigma(\pi A \rightarrow X), \quad (13)$$

as could be anticipated in accordance with the Adler relation. Notice that the high-energy regime actually starts at rather low energies if $Q^2 \lesssim m_\pi^2$.

The results of numerical evaluation of the shadowing effect Eq. (12) for neon are plotted in Fig. 3. The calculations [10] done within the Glauber approximation, Eq. (12), and also

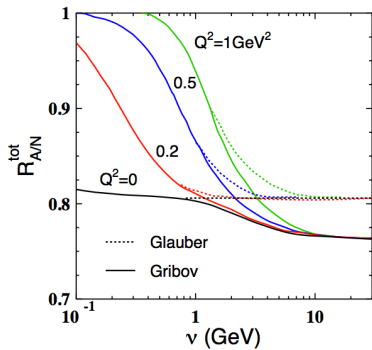


FIG. 3: The neon to nucleon ratio of total neutrino cross sections at different Q^2 [10]. Dashed and solid curves correspond to the Glauber and Gribov corrected calculations.

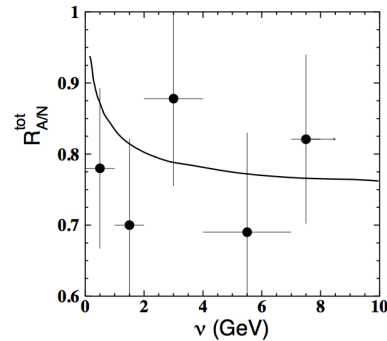


FIG. 4: The neon to proton ratio of the total neutrino cross sections, calculated in Ref.[10] for $x < 0.2$ and $Q^2 < 0.2 \text{ GeV}^2$. The data present the BEBC results [11].

including the Gribov's inelastic corrections (important at high energies $\nu > m_{a_1}^2 R_A$) are plotted in Fig. 3 by solid curves as function of energy, for different Q^2 .

The calculated shadowing effects are compared with BEBC data [11] in Fig. 4. As was anticipated, the shadowing exposes an early onset, and a significant suppression occurs at small Q^2 in the low energy range of hundreds MeV. This is an outstanding feature of the axial current. This seems to be supported by data, although with a rather poor statistics.

Concluding this section, we notice that although the approximation of lowest order Gribov corrections does in some cases good job, the higher order off-diagonal transitions

neglected in (11) and (12), might be important, but unknown. Indeed, the intermediate state X has definite mass M , but no definite cross section. It was fixed in (11) at σ_{tot}^{hN} with no justification.

Thus, the lowest order Gribov correction Eq. (11) has a nice feature of including phase shifts, which allows to describe the onset of Gribov shadowing, like is presented in Fig. 2. However, the uncertainties related to the missed higher order corrections and the unknown absorption in (11) seem to be incurable, while one works in the hadronic (eigenstates of the mass matrix) representation.

A. Interaction eigenstate representation

If a hadron were an eigenstate of interaction, i.e. could undergo only elastic scattering (as a shadow of inelastic channels) and no diffractive excitation was possible, the Glauber formula would be exact and no inelastic shadowing corrections were needed. This simple observation gives a hint that one should switch from the hadronic basis to a complete set of mutually orthogonal eigenstates of the scattering amplitude operator. This was the driving idea of the description of diffraction in terms of elastic amplitudes [12, 13], and becomes a powerful tool for calculation of inelastic shadowing corrections in all orders of multiple interactions [14, 15]. Notice that this idea also was used by Gribov [2] to explain the role of the coherence length increasing with energy, on the example of an incoming proton, fluctuating to a nucleon-pion pair.

Physical states (including leptons, photons) can be expanded over the complete set of states $|k\rangle$,

$$|h\rangle = \sum_k \Psi_k^h |k\rangle, \quad (14)$$

which are the eigenstates of the scattering amplitude operator, $\hat{f}|k\rangle = f_{el}^{kN}|k\rangle$. For the sake of simplicity we neglect the real part of the amplitude, i.e. assume that $f_{el}^{kN} = i\sigma_{tot}^{kN}/2$.

Ψ_k^h in (14) are weight factors (amplitudes) of the Fock state decomposition. They obey the orthogonality conditions,

$$\begin{aligned} \sum_k (\Psi_k^{h'})^\dagger \Psi_k^h &= \delta_{hh'}; \\ \sum_h (\Psi_h^l)^\dagger \Psi_h^k &= \delta_{lk}. \end{aligned} \quad (15)$$

We also assume that the amplitude is integrated over impact parameter, *i.e.* that the forward elastic amplitude is normalized as $|f_{el}^{kN}|^2 = 4\pi d\sigma_{el}^{kN}/dt|_{t=0}$. The amplitudes of elastic $f_{el}(hh)$ and off diagonal diffractive $f_{sd}(hh')$ transitions can be expressed as,

$$f_{el}^{hN} = 2i \sum_k |\Psi_k^h|^2 \sigma_{tot}^{kN} \equiv 2i \langle \sigma \rangle; \quad (16)$$

$$f_{sd}^{hN}(h \rightarrow h') = 2i \sum_k (\Psi_k^{h'})^\dagger \Psi_k^h \sigma_{tot}^{kN}. \quad (17)$$

Note that if all the eigenamplitudes were equal, the diffractive amplitude (17) would vanish due to the orthogonality relation, (15). The physical reason is obvious. If all the f_{el}^{kN} are

equal, the interaction does not affect the coherence between different eigen components $|k\rangle$ of the projectile hadron $|h\rangle$. Therefore, the off-diagonal transitions are possible only due to differences between the eigenamplitudes.

By summing up in the diffractive cross section using completeness Eq. (15), and excluding the elastic channels, one gets [14–16],

$$\begin{aligned} 16\pi \left. \frac{d\sigma_{sd}^{hN}}{dt} \right|_{t=0} &= \sum_k |\Psi_k^h|^2 (\sigma_{tot}^{kN})^2 - \left(\sum_i |\Psi_i^h|^2 \sigma_{tot}^{kN} \right)^2 \\ &\equiv \langle (\sigma_{tot}^{kN})^2 \rangle - \langle \sigma_{tot}^{kN} \rangle^2 . \end{aligned} \quad (18)$$

Each of the eigenstates propagating through the nucleus can experience only elastic scatterings, so the Glauber eikonal approximation becomes exact for such a state. Then, the cross sections for hadron-nucleus collisions should be averaged over the Fock states, chosen to be interaction eigenstates [14, 15],

$$\sigma_{tot}^{hA} = 2 \int d^2b \left\{ 1 - \left\langle \exp \left[-\frac{1}{2} \sigma_{tot}^{kN} T_A^h(b) \right] \right\rangle \right\}. \quad (19)$$

This is to be compared with the Glauber approximation. The difference is obvious, in Eq. (19) the exponential is averaged, while in the Glauber approximation the exponent is averaged,

$$\sigma_{tot}^{hA} \Big|_{Gl} = 2 \int d^2b \left\{ 1 - \exp \left[-\frac{1}{2} \langle \sigma_{tot}^{kN} \rangle T_A^h(b) \right] \right\}, \quad (20)$$

where $\langle \sigma_{tot}^{kN} \rangle = \sigma_{tot}^{hN}$. The difference between Eqs. (19) and (20), is the Gribov inelastic correction calculated in all orders of opacity expansion, which was impossible to do within hadronic representation (see above). This result can be compared with the expression (11) for the lowest order correction expanding the exponentials in (19) and (20) in number of collisions up to the lowest order. Applying (18) we find,

$$\begin{aligned} \sigma_{tot}^{hA} - \sigma_{tot}^{hA} \Big|_{Gl} &= \int d^2b \frac{1}{4} \left[\langle \sigma_{tot}^{kN} \rangle^2 - \langle (\sigma_{tot}^{kN})^2 \rangle \right] T_A^h(b)^2 \\ &= -4\pi \int d^2b T_A^h(b)^2 \int dM^2 \left. \frac{d\sigma_{sd}^h}{dM^2 dt} \right|_{t=0}. \end{aligned} \quad (21)$$

This result is indeed identical to Eq. (11), if to neglect the phase shift vanishing at high energies, and also to expand the exponential.

III. COLOR DIPOLES AS EIGENSTATES OF INTERACTIONS

The dipole representation in QCD, first proposed in Ref.[15], allows to calculate Gribov corrections in all orders, because a high energy dipole is an eigenstate of interaction. Indeed, the transverse dipole separation, which controls the scattering amplitude, is preserved during propagation and remains intact after multiple soft interactions within a nuclear target.

To perform proper averaging in (19) one should expand the beam particle (hadrons, vector or axial currents) over Fock states. Each Fock component is a colorless dipole, consisted of two or more partons. After averaging over intrinsic dipole distances, one should sum up different Fock states with proper weights.

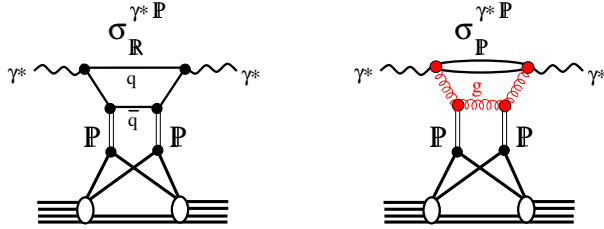


FIG. 5: Gribov corrections with $\bar{q}q$ and $\bar{q}q + g$ intermediate states.

A. Deep-inelastic scattering

The parton model interpretation of the space-time development of reactions is not Lorentz invariant. While Deep-inelastic scattering (DIS) at small $x \ll 1$ is interpreted in the Bjorken reference frame as absorption of the virtual photon by a target parton carrying corresponding fractional momentum x of the target, in the target rest frame it looks differently. The high energy virtual photon fluctuates into a $\bar{q}q$ pair, which interacts with the targets and is produced on mass shell.

The two main contributions to the diffractive cross section in (11) at high energies come from the triple-Regge terms $\mathbb{P}\mathbb{P}\mathbb{R}$ and $\mathbb{P}\mathbb{P}\mathbb{P}$, which generate $1/M^3$ and $1/M^2$ mass dependences respectively. The quark-gluon structure of these contributions in diffraction is illustrated in Fig. 5. Apparently, the $\bar{q}q$ and $\bar{q}qg$ states, propagating through the nucleus, attenuate with an absorptive cross section, which cannot be trivially fixed, like was done in (11), but should be properly treated within the dipole approach.

1. "Frozen" dipoles

If the lifetime of partonic fluctuations of a photon significantly exceeds the nuclear size, the dipole approach allows to calculate easily the shadowing effects in DIS. Indeed, in this case one can rely on the "frozen" approximation Eq. (19), which for interaction of a virtual photon has the form,

$$\begin{aligned} \sigma_{T,L}^{\gamma^*A}(x, Q^2) &= 2 \int d^2b \int_0^1 d\alpha \int d^2r_T \left| \Psi_{q\bar{q}}^{T,L}(\alpha, r_T, Q^2) \right|^2 \\ &\times \left[1 - e^{-\frac{1}{2}\sigma_{q\bar{q}}(r_T, x)T_A(b)} \right], \end{aligned} \quad (22)$$

where r_T is the dipole transverse separation; α is the fractional light-cone momentum of the quark; the distribution functions $\Psi_{q\bar{q}}^{T,L}(\alpha, r_T)$ in the quadratic form read,

$$\begin{aligned} \left| \Psi_{q\bar{q}}^T(\alpha, r_T) \right|^2 &= \frac{2N_c\alpha_{em}}{(2\pi)^2} \sum_{f=1}^{N_f} Z_f^2 \{ [1 - 2\alpha(1 - \alpha)] \varepsilon^2 K_1^2(\varepsilon r_T) \\ &+ m_f^2 K_0^2(\varepsilon r_T) \}; \end{aligned} \quad (23)$$

$$\left| \Psi_{q\bar{q}}^L(\alpha, r_T) \right|^2 = \frac{8N_c\alpha_{em}}{(2\pi)^2} \sum_{f=1}^{N_f} Z_f^2 Q^2 \alpha^2 (1 - \alpha)^2 K_0^2(\varepsilon r_T). \quad (24)$$

The advantage of the dipole description is pretty obvious, Eq. (22) includes Gribov inelastic shadowing corrections to all orders of multiple interactions [15], what is hardly possible within hadronic representation.

On the other hand, the dipoles having a definite size, do not have any definite mass, therefore the phase shifts between amplitudes on different nucleons cannot be calculated as simple as in Eq. (11). A solution for this problem was proposed in Ref.[17, 18].

2. Path integral technique

The lifetime of the "frozen" dipole, or coherence length (or time), is given by,

$$l_c = \frac{2\nu}{Q^2 + M_{\bar{q}q}^2}, \quad (25)$$

where ν is the dipole energy in the target rest frame; $M_{\bar{q}q}^2 = (m_q^2 + k_T^2)/\alpha(1 - \alpha)$. At very small Bjorken $x = Q^2/2m_N\nu \ll 1$ the coherence length can significantly exceed the nuclear size, $l_c \gg R_A$, and one can safely rely on the "frozen" approximation. However, if $t_c \lesssim R_A$ such an approximation is not appropriate and one should correct for the dipole size fluctuations during propagation through the nucleus, which corresponds to inclusion of the phase shifts between DIS amplitudes on different bound nucleons in Eq. (11). Within the dipole description this can be done employing the path integral technique [19], which sums up different propagation paths of the partons.

For a $\bar{q}q$ component of a transversely or longitudinally polarized virtual photon Eq. (22) should be replaced by,

$$\begin{aligned} \left(\sigma_{tot}^{\gamma^*A}\right)^{T,L} &= A\left(\sigma_{tot}^{\gamma^*N}\right)^{T,L} \\ &- \frac{1}{2}Re \int d^2b \int_0^1 d\alpha \int_{-\infty}^{\infty} dz_1 \int_{z_1}^{\infty} dz_2 \int d^2r_1 \int d^2r_2 \\ &\times \Psi_{\bar{q}q}^{T,L\dagger}(\varepsilon, \vec{r}_2) \rho_A(b, z_2) \sigma_{q\bar{q}}^N(s, \vec{r}_2) G(\vec{r}_2, z_2 | \vec{r}_1, z_1) \\ &\times \rho_A(b, z_1) \sigma_{q\bar{q}}^N(s, \vec{r}_1) \Psi_{\bar{q}q}^{T,L}(\varepsilon, \vec{r}_1). \end{aligned} \quad (26)$$

The Green's function $G(\vec{r}_2, z_2 | \vec{r}_1, z_1)$ describes propagation of a $\bar{q}q$ pair in an absorptive medium, having initial separation \vec{r}_1 at the initial position z_1 , up to the point z_2 , where it gets separation \vec{r}_2 , as is illustrated in Fig. 6.

It satisfies the evolution equation [18, 20, 21],

$$\left[i \frac{\partial}{\partial z_2} + \frac{\Delta_{\perp}(r_2) - \varepsilon^2}{2\nu\alpha(1 - \alpha)} + U(r_2, z_2) \right] G(\vec{r}_2, z_2 | \vec{r}_1, z_1) = 0 \quad (27)$$

The light-cone potential in the left-hand side of this equation describes nonperturbative interactions within the dipole, and its absorption in the medium. The real part the potential responsible for nonperturbative quark interactions was modelled and fitted to data of F_2^p in Ref.[34]. Here we fix $\text{Re} U(r_2, z_2) = 0$, and treat quarks as free particles for the sake of simplicity. The imaginary part of the potential describes the attenuation of the dipole in the medium,

$$\text{Im} U(r, z) = -\frac{1}{2} \sigma_{\bar{q}q}(r) \rho_A(b, z). \quad (28)$$

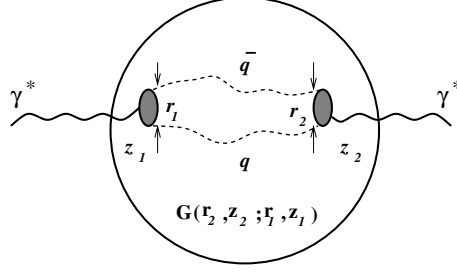


FIG. 6: Propagation of a $q\bar{q}$ -pair through a nucleus between points with longitudinal coordinates z_1 and z_2 . The evolution of the $\bar{q}q$ separation from the initial, \vec{r}_1 , up to the final, \vec{r}_2 , due to the transverse motion of the quarks, is described by the Green's function $G(\vec{\rho}_2, z_2; \vec{\rho}_1, z_1)$, a solution of Eq. (27).

The numerical results of the calculations, which are performed either disregarding or including the real part of the potential, modelled in Ref.[34], are plotted in Fig. 7 by dashed and solid curves respectively. One can see that inclusion of the nonperturbative effects does not lead to a significant change of the magnitude of shadowing. Comparison with NMC data [23, 24] shows pretty good agreement. We remind that this is a parameter-free description.

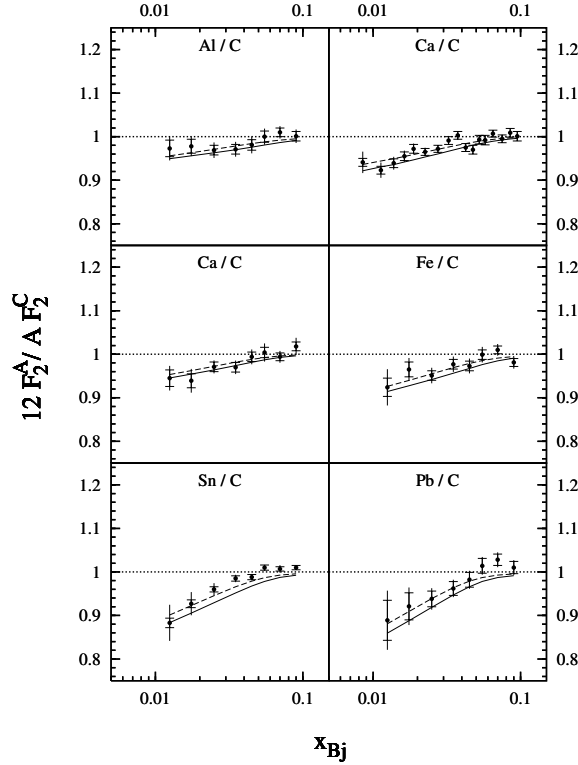


FIG. 7: Comparison between calculations for shadowing in DIS and experimental data from NMC [23, 24] for the structure functions of different nuclei relative to carbon. Q^2 ranges within $3 \leq Q^2 \leq 17 \text{ GeV}^2$. The solid and dashed curves are calculated including or excluding the real part of the potential respectively.

More example of comparison with data can be found in Ref.[22]. Notice also that we did not

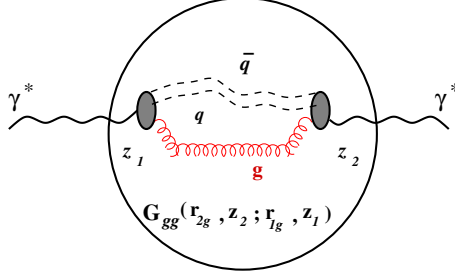


FIG. 8: Propagation through a nucleus of the $q\bar{q} - g$ fluctuation of a longitudinally polarized photon. Neglecting the small, $\sim 1/Q^2$ size of the color-octet $\bar{q}q$ pair, the effective octet-octet dipole propagation is described by the Green's function $G_{gg}(\vec{r}_{2g}, z_2; \vec{r}_{1g}, z_1)$.

include any mechanism of nuclear enhancement at $x > 0.1$, the effect called antishadowing, which affect the small- x region as well.

3. Gluon shadowing

As was mentioned above, the contribution of all Fock components in the cross section should be summed up

$$\sigma_{tot}^{\gamma^*A} = A \sigma_{tot}^{\gamma^*N} - \Delta\sigma_{tot}(\bar{q}q) - \Delta\sigma_{tot}(\bar{q}qg) - \Delta\sigma_{tot}(\bar{q}q2g) - \dots \quad (29)$$

The next after the $\bar{q}q$ Fock component is $\bar{q}q + g$. It has a considerably shorter coherence time, compared with $\bar{q}q$, because of specific nonperturbative effects increasing the mean transverse momentum of gluons [25, 34]. Correspondingly, the next component $|\bar{q}q2g\rangle$ has even a much shorter coherence time t_c , which makes the 4th term in (29) negligibly small within the currently achieved kinematic range. Thus, we keep only first two low Fock components.

Notice that a successful attempt to sum up all Fock components was done in the form of Balitsky-Kovchegov equation [26, 27]

The 3rd term in the total cross section Eq. (29) is illustrated in Fig. 8.

Differently from the case of a $|\bar{q}q\rangle$ Fock state, where we found that at high Q^2 perturbative QCD can be safely used for shadowing calculations, the nonperturbative effects remain important for the $|\bar{q}qg\rangle$ component even for highly virtual photons. High Q^2 squeezes the $\bar{q}q$ pair down to a size $\sim 1/Q$, while the mean quark-gluon separation at $\alpha_g \ll 1$ depends on the strength of nonperturbative gluon interaction which is characterised in this limit by a small separation $r_0 \approx 0.3$ fm [34]. which considerably smaller than the confinement radius $1/\Lambda_{QCD}$. This is confirmed by various experimental observations [25], in particular by the observed strong suppression of the diffractive gluon radiation [34]. In nonperturbative QCD models this scale is related to the instanton size [28, 29].

The nonperturbative quark-gluon wave function was found in Ref.[34] to have the form,

$$\Psi_{qg}(\vec{r}_g, \alpha_g) \Big|_{\alpha_g \ll 1} = -\frac{2i}{\pi} \sqrt{\frac{\alpha_s}{3}} \frac{\vec{e} \cdot \vec{r}_g}{r_g^2} \exp\left(-\frac{r_g^2}{2r_0^2}\right), \quad (30)$$

where \vec{e} is the gluon polarization vector.

For $Q^2 \gg 1/r_0^2$ the $\bar{q}q$ is small, $r_{\bar{q}q}^2 \ll r_g^2$, and one can treat the $\bar{q}qg$ system as a color octet-octet dipole, as is illustrated in Fig. 8. Then the three-body Green's function factorizes,

$$G_{q\bar{q}g}(\vec{r}_{2g}, \vec{r}_2, z_2; \vec{r}_{1g}, \vec{r}_1, z_1) \Rightarrow G_{q\bar{q}}(\vec{r}_2, z_2; \vec{r}_1, z_1) G_{gg}(\vec{r}_{2g}, z_2; \vec{r}_{1g}, z_1). \quad (31)$$

The color octet-octet Green function G_{gg} , describing the propagation of a glue-gluon dipole with $\alpha_g \ll 1$ through the medium, satisfies the simplified evolution equation [34],

$$\left[i \frac{\partial}{\partial z_2} - \frac{Q^2}{2\nu} - V(\vec{r}_{2g}, z_2) \right] G_{gg}(\vec{r}_{2g}, z_2; \vec{r}_{1g}, z_1) = 0 \quad (32)$$

Here

$$\text{Im } V(\vec{r}_{2g}, z) = -\frac{1}{2} \sigma_{gg}(r, x) \rho_A(z), \quad (33)$$

with the color-octet dipole cross section, which reads,

$$\sigma_{gg}(r, x) = \frac{9}{4} \sigma_{q\bar{q}}(r, x). \quad (34)$$

The real part of the potential must correctly reproduce the wave function Eq. (30).

$$\text{Re } V(\vec{r}_{2g}, z) = \frac{r_{2g}^2}{2\nu\alpha_g r_0^4} \quad (35)$$

Longitudinal photons can be used to disentangle between the effects of higher twist quark shadowing (2d term in (29)), and leading twist gluon shadowing (3rd term in (29)). The contribution, which mixes up these two types of Gribov corrections, come from so called aligned jet configurations [30] of the $\bar{q}q$ pair. Namely the mean $\bar{q}q$ separation $r_{\bar{q}q}^2 \sim Q^2/\alpha_q(1-\alpha_q)$ is small, unless the large value of Q^2 is compensated by smallness of α_q or $(1-\alpha_q)$. In the wave function of longitudinal photons, Eq. (24) such aligned-jet configurations are suppressed, so shadowing of longitudinal photons should represent the net effect of gluon shadowing.

While the distance between the q and the \bar{q} is small, of order $1/Q^2$, the gluon can propagate relatively far at a distance $r_g \sim r_0$ from the $q\bar{q}$ -pair, which after the emission of the gluon is in a color-octet state. Therefore, the entire $|q\bar{q}g\rangle$ -system appears as a octet-octet gg -dipole, and the shadowing correction to the longitudinal cross section directly gives the magnitude of gluon shadowing, which we want to calculate.

Thus, the cross section of longitudinal photons is proportional to the gluon distribution function, therefore,

$$\frac{g_A(x, Q^2)}{g_N(x, Q^2)} \approx \frac{\sigma_A^L(x, Q^2)}{\sigma_N^L(x, Q^2)} \quad (36)$$

The shadowing correction to $\sigma_A^L(x, Q^2)$ has the form (compare with (26)),

$$\begin{aligned} \Delta\sigma_A^L(x, Q^2) &= -\text{Re} \int d^2b \int_{-\infty}^{\infty} dz_1 \int_{z_1}^{\infty} dz_2 \rho_A(b, z_1) \rho_A(b, z_2) \\ &\times \int d^2r_{2g} d^2r_{2\bar{q}q} d^2r_{1g} d^2r_{1\bar{q}q} \int d\alpha_q d\ln(\alpha_g) F_{\gamma^* \rightarrow \bar{q}qg}^\dagger(\vec{r}_{2g}, \vec{r}_{2\bar{q}q}, \alpha_q, \alpha_g) \\ &\times G_{\bar{q}qg}(\vec{r}_{2g}, \vec{r}_{2\bar{q}q}, z_2; \vec{r}_{1g}, \vec{r}_{1\bar{q}q}, z_1) F_{\gamma^* \rightarrow \bar{q}qg}(\vec{r}_{1g}, \vec{r}_{1\bar{q}q}, \alpha_q, \alpha_g) \end{aligned} \quad (37)$$

Here

$$F_{\gamma^* \rightarrow \bar{q}qg}^\dagger(\vec{r}_g, \vec{r}_{\bar{q}q}, \alpha_q, \alpha_g) = -\Psi_{\bar{q}q}^L(\vec{r}_{\bar{q}q}, \alpha_q) \vec{r}_g \cdot \vec{\nabla} \Psi_{qg}(\vec{r}_g) \sigma_{gg}^N(x, r_g) , \quad (38)$$

Assuming $Q^2 \gg 1/r_0^2$ we can neglect $r_{\bar{q}q} \ll r_g$. The net diffractive amplitude $F_{\gamma^* \rightarrow \bar{q}qg}(\vec{r}_{1g}, \vec{r}_{1\bar{q}q}, \alpha_q, \alpha_g)$ takes the form of Eq. (38), and we can rely on the factorized relation (31) for the 3-body Green's function, with equation (32) for the evolution of the gluonic dipole.

The results of numerical calculation of (37) for the ratio

$$R_g(x, Q^2) = \frac{g_A(x, Q^2)}{A g_N(x, Q^2)}, \quad (39)$$

are depicted in Fig. 9 as function of Bjorken x for $Q^2 = 4$ and 40 GeV^2 . The predicted small

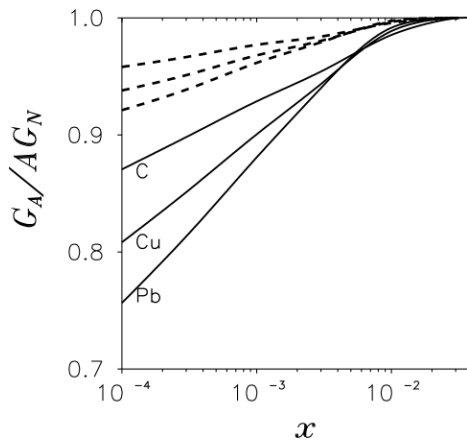


FIG. 9: Ratio (39) for carbon, copper and lead at small Bjorken x and $Q^2 = 4 \text{ GeV}^2$ (solid curves) and 40 GeV^2 (dashed curves).

magnitude of gluon shadowing was confirmed by next-to-leading (NLO) global analyses of DIS data [31, 32]. It also goes along with the well known smallness of the triple-Pomeron coupling, measured at low virtuality [33]. The latter controls large mass diffraction, which proceeds via gluon radiation, and its smallness leads to suppression of gluon radiation and gluon shadowing related to corresponding Gribov corrections. The observed weakness of these effects is interpreted in the dipole approach a smallness of the parameter $r_0 \approx 0.3 \text{ fm}$ in Eq. (30) [25, 34].

B. Hadron-nucleus cross sections

Applications of the dipole approach to calculation of Gribov corrections to the hadron-nucleus total cross sections contains more uncertainties and modelling compared with hard reactions, like DIS. Nevertheless, it allows to make a progress compared with the hadronic representation, which involves ad hoc assumptions about the interaction cross section, of an excited hadronic state, and the unknown higher terms in the opacity expansion.

1. *Excitation of the valence quark skeleton of the proton*

First of all one should rely on a parametrization of the dipole cross section, which allows an extension to the soft, large separation region. Following [5, 34] we chose the saturated shape of the cross section, which rises as r_T^2 at small r_T , but levels off at large r_T ,

$$\sigma_{\bar{q}q}(r_T, s) = \sigma_0(s) \left[1 - \exp\left(-\frac{r_T^2}{R_0^2(s)}\right) \right], \quad (40)$$

where $R_0(s) = 0.88 fm (s_0/s)^{0.14}$ and $s_0 = 1000 GeV^2$ [34]. The energy dependent factor $\sigma_0(s)$ is defined as,

$$\sigma_0(s) = \sigma_{tot}^{\pi p}(s) \left(1 + \frac{3 R_0^2(s)}{8 \langle r_{ch}^2 \rangle_\pi} \right), \quad (41)$$

where $\langle r_{ch}^2 \rangle_\pi = 0.44 \pm 0.01 fm^2$ [37] is the mean square of the pion charge radius.

This dipole cross section is normalized to reproduce the pion-proton total cross section, $\langle \sigma_{\bar{q}q} \rangle_\pi = \sigma_{tot}^{\pi p}(s)$. The saturated shape of the dipole cross section is inspired by the popular parametrization given in Ref. [35, 36], which is fitted to the low- x and high Q^2 data for $F_2^p(x, Q^2)$ from HERA. However, that should not be used for our purpose, since is unable to provide the correct energy dependence of hadronic cross sections. Namely, the pion-proton cross section cannot exceed 23mb. Besides, Bjorken x is not a proper variable for soft reactions, since at small Q^2 the value of x is large even at low energies. The s -dependent dipole cross section Eq. (40) was fitted [34] to data for hadronic cross sections, real photoproduction and low- Q^2 HERA data for the proton structure function. The cross section (41) averaged with the pion wave function squared (see below) automatically reproduces the pion-proton cross section.

In the case of a proton beam one needs a cross section for a three-quark dipole, $\sigma_{3q}(\vec{r}_1, \vec{r}_2, \vec{r}_3)$, where \vec{r}_i are the transverse quark separation with a condition $\vec{r}_1 + \vec{r}_2 + \vec{r}_3 = 0$. In order to avoid the introduction of a new unknown phenomenological quantity, we express the three-body dipole cross section via the conventional dipole cross section $\sigma_{\bar{q}q}$ [4],

$$\sigma_{3q}(\vec{r}_1, \vec{r}_2, \vec{r}_3) = \frac{1}{2} \left[\sigma_{\bar{q}q}(r_1) + \sigma_{\bar{q}q}(r_2) + \sigma_{\bar{q}q}(r_3) \right]. \quad (42)$$

This form satisfies the limiting conditions, namely, turns into $\sigma_{\bar{q}q}(r)$ if one of three separations is zero. Since all these cross sections involve nonperturbative effects, this relation hardly can be proven, but should be treated as a plausible assumption.

The 3-quark valence wave function is modelled assuming that the dipole cross section is independent of the sharing of the light-cone momentum among the quarks, so the wave function squared of the valence Fock component of the proton, $|\Phi(\vec{r}_i, \alpha_j)|^2$ should be integrated over fractions α_i . The result depends only on transverse separations \vec{r}_i . The form of the nonperturbative valence quark distribution is unknown, therefore for the sake of simplicity we assume the Gaussian form,

$$\begin{aligned} |\Psi_N(\vec{r}_1, \vec{r}_2, \vec{r}_3)|^2 &= \int_0^1 \prod_{i=1}^3 d\alpha_i |\Phi(\vec{r}_i, \alpha_j)|^2 \delta\left(1 - \sum_{j=1}^3 \alpha_j\right) \\ &= \frac{2 + r_p^2/R_p^2}{(\pi r_p R_p)^2} \exp\left(-\frac{r_1^2}{r_p^2} - \frac{r_2^2 + r_3^2}{R_p^2}\right) \delta(\vec{r}_1 + \vec{r}_2 + \vec{r}_3), \end{aligned} \quad (43)$$

where \vec{r}_i are the interquark transverse distances. The two scales r_p and R_p characterizing the mean transverse size of a diquark and the mean distances to the third quark.

For the sake of simplicity here we assume that the forces binding the valence quarks are of an iso-scalar nature, therefore the quark distribution is symmetric, i.e. $r_p = R_p$ in (43). In this case the mean interquark separation squared is $\langle \vec{r}_i^2 \rangle = \frac{2}{3} R_p^2 = 2 \langle r_{ch}^2 \rangle_p$. See other possibilities of an asymmetric valence structure in Ref.[5].

Apparently, any model for the dipole cross section and valence quark distribution in the proton, must reproduce correctly data for diffractive excitation of the proton, otherwise the Gribov corrections will come out wrong. It was demonstrated that with the above choice of the dipole cross section and proton wave function one reproduces quite well the results of the global analysis [33] of single diffraction data, namely the triple-Reggeon term \mathbb{PPR} , as well as the triple-Pomeron one \mathbb{PPP} , controlling diffractive gluon radiation.

Now we are in a position to calculate the Gribov corrections.

2. Excitation of the valence quark skeleton of the proton

The total cross sections reads,

$$\begin{aligned} \sigma_{tot}^{pA} &= 2 \int d^2b \left[1 - \left\langle e^{-\frac{1}{2} \sigma_{3q}(r_i) T_A(b)} \right\rangle \right] \\ &\equiv 2 \int d^2b \left[1 - \int \prod_{i=1}^3 d^2r_i |\Psi_N(r_j)|^2 e^{-\frac{1}{2} \sigma_{3q}(\vec{r}_k) T_A(b)} \right]. \end{aligned} \quad (44)$$

Using the wave function Eq. (43) with $r_p = R_p$ and the cross section (40) we get the following forward elastic cross section,

$$\left. \frac{d\sigma_{el}^{pp}}{dp_T^2} \right|_{p_T=0} = \frac{\gamma^2}{(1 + \frac{2}{3}\gamma)^2} \frac{\sigma_0^2(s)}{16\pi}, \quad (45)$$

where $\gamma = 3 \langle r_{ch}^2 \rangle_p / R_0^2(s)$.

IV. GLUON SHADOWING

Eikonalization of the lowest Fock state $|3q\rangle$ of the proton done in (44) corresponds to the Bethe-Heitler regime of gluon radiation. Indeed, gluon bremsstrahlung is responsible for the rising energy dependence of the cross section, and in the eikonal form (44) one assumes that the whole spectrum of gluons is radiated in each of multiple interactions. However, the Landau-Pomeranchuk-Migdal effect [38, 39] is known to suppress radiation in multiple interactions. Since a substantial part of the inelastic cross section at high energies is related to gluon radiation, the LPM effect suppresses the cross section. This is a quantum-mechanical interference phenomenon and it is a part of the suppression called Gribov inelastic shadowing. In the QCD dipole picture it come from inclusion of higher Fock states, $|3qg\rangle$, etc. Each of these states represents a colorless dipole and its elastic amplitude on a nucleon is subject to eikonalization.

As we already mentioned, the eikonalization procedure requires the fluctuation lifetime to be much longer than the nuclear size. Otherwise, one has to take into account the

”breathing” of the fluctuation during propagation through a nucleus, which can be done by applying the light-cone Green function technique [20, 21, 34]. In hadronic representation this is equivalent to saying that all the longitudinal momenta transfers must be much smaller than the inverse mean free path of the hadron in the nucleus. Otherwise, one should employ the path-integral technique, described above.

The c.m. energies of HERA-B, RHIC and LHC are sufficiently high to treat the lowest Fock state containing only valence quarks as ”frozen” by the Lorentz time dilation during propagation through the nucleus. Indeed, for the excitations with the typical nucleon resonance masses, the coherence length is sufficiently long compared to the nuclear size. This is why we applied eikonalization without hesitation so far. Such an approximation, however, never works for the higher Fock states containing gluons. Indeed, since the gluon is a vector particle, the integration over effective mass of the fluctuation is divergent, dM^2/M^2 , which is the standard triple-Pomeron behaviour. Therefore, the energy of collisions can never be sufficiently high to neglect the large-mass tail. For this reason the inelastic shadowing corrections, related to excitation gluonic degrees of freedom never saturates, and keeps rising logarithmically with energy.

There are, however non-linear effects which are expected to stop the rise of inelastic corrections at high energies. This is related to the phenomenon of gluon saturation [40, 41] or color glass condensate [42]. The strength of these nonlinear effect is expected to be rather mild due to smallness of the gluonic spots in the nucleus [25]. The reason is simple, in spite of a sufficient longitudinal overlap of gluon clouds originated from different nucleons, there is insufficient overlap in the transverse plane. This fact leads to a delay of the onset of saturation up to very high energies, since the transverse radius squared of the gluonic clouds rise with energy very slowly, logarithmically, with a small coefficient of the order of 0.1 GeV^{-2} .

The details of the calculation of inelastic corrections related to excitation of gluonic degrees of freedom can be found in Ref.[4, 34]. The numerical results for nuclear cross sections at the energies of RHIC and LHC can be found in Ref.[5, 6]. As an example, the total proton-lead cross section, calculated at $\sqrt{s} = 5 \text{ TeV}$ in the Glauber approximation, and corrected to Gribov shadowing related to excitation of valence quarks and gluons, results in $\sigma_{tot}^{pPb} = 4242.5 \text{ mb}$; 4235.2 mb ; and 4207.1 mb respectively.

V. SUMMARY

The dipole phenomenology in QCD has been intensively developing over the past three decades, due to both theoretical efforts and precise experimental data, in particular from HERA. This theoretical tool allows to calculate the effects of Gribov inelastic shadowing on a more solid ground and in all orders of opacity expansion. In this note we presented several explicit examples.

Acknowledgements: Work was partially supported by Fondecyt (Chile) grant 1130543.

-
- [1] R. J. Glauber, in *Lectures in Theoretical Physics*, Editors: W. E. Brittin *et al.* (New York, 1959).
- [2] V. N. Gribov, *Sov. Phys. JETP* **29**, 483 (1969) [*Zh. Eksp. Teor. Fiz.* **56**, 892 (1969)];
- [3] V. N. Gribov, *Sov. Phys. JETP* **30**, 709 (1970) [*Zh. Eksp. Teor. Fiz.* **57**, 1306 (1970) 1306].
- [4] B. Z. Kopeliovich, *Phys. Rev.* **C68**, 044906 (2003).
- [5] B. Z. Kopeliovich, I. K. Potashnikova and I. Schmidt, *Phys. Rev.* **C73**, 034901 (2006).
- [6] M. Alvioli, C. Ciofi degli Atti, B. Z. Kopeliovich, I. K. Potashnikova and I. Schmidt, *Phys. Rev.* **C81**, 025204 (2010).
- [7] V. Karmanov and L.A. Kondratyuk, *Sov. Phys. JETP Lett.* **18**, 266 (1973).
- [8] P.V.R. Murthy *et al.*, *Nucl. Phys.* **B 92**, 269 (1975).
- [9] A. Gsponer *et al.*, *Phys. Rev. Lett.* **42**, 9 (1979).
- [10] B. Z. Kopeliovich, *Phys. Lett.* **B227**, 461 (1989).
- [11] P.P. Allport *et al.* [WA59 Collaboration], *Phys. Lett.* **B232**, 417 (1989).
- [12] E. Feinberg and I.Ya. Pomeranchuk, *Nuovo. Cimento. Suppl.* **3**, 652 (1956).
- [13] M.L. Good and W.D. Walker, *Phys. Rev.* **120**, 1857 (1960).
- [14] B.Z. Kopeliovich and L.I. Lapidus, *Sov. Phys. Sov. Phys. JETP Lett.* **28**, 664 (1978).
- [15] B. Z. Kopeliovich, L. I. Lapidus and A. B. Zamolodchikov, *JETP Lett.* **33**, 595 (1981).
- [16] H.I. Miettinen and J. Pumplin, *Phys. Rev.* **D18**, 1696 (1978).
- [17] B.Z. Kopeliovich, J. Raufeisen and A.V. Tarasov, *Phys. Lett.* **B440**, 151 (1998).
- [18] B. G. Zakharov, *Phys. Atom. Nucl.* **61**, 838 (1998).
- [19] R. Feynman and A.R. Hibbs, *Quantum mechanics and path integrals* (McGraw-Hill, New York, 1965).
- [20] B. Z. Kopeliovich and B.G. Zakharov, *Phys. Rev.* **D44**, 3466 (1991).
- [21] B. Z. Kopeliovich, A. Schäfer, and A. V. Tarasov, *Phys. Rev.* **C59**, 1609 (1999). See the extended version in hep-ph/9808378.
- [22] B.Z. Kopeliovich, J. Raufeisen and A.V. Tarasov, *Phys. Rev.* **C6 2**, 035204 (2000).
- [23] The NM Coll., M. Arneodo *et al.* *Nucl. Phys.* **B481**, 23 (1996).
- [24] NM Collab., P. Amaudruz *et al.* *Nucl. Phys.* **B441**, 3 (1995).
- [25] B. Z. Kopeliovich, I. K. Potashnikova, B. Povh, I. Schmidt, *Phys. Rev.* **D76** , 094020 (2007).
- [26] I. Balitsky, *Nucl. Phys.* **B463**, 99 (1996).
- [27] Y. V. Kovchegov, *Phys. Rev.* **D60**, 034008 (1999).
- [28] T. Schäfer and E.V. Shuryak, *Rev. Mod. Phys.* **70**, 323 (1998).
- [29] E. Shuryak and I. Zahed, *Phys. Rev.* **D69**, 014011 (2004).
- [30] J. D. Bjorken and J. Kogut, *Phys. Rev.* **D8**, 1341 (1973).
- [31] D. de Florian and R. Sassot, *Phys. Rev.* **D69**, 074028 (2004).
- [32] M. Hirai, S. Kumano and T.-H. Nagai, *Phys. Rev.* **C70**, 044905 (2004).
- [33] Y. .M. Kazarinov, B. Z. Kopeliovich, L. I. Lapidus, I. K. Potashnikova, *JETP* **43** , 598 (1976).
- [34] B. Z. Kopeliovich, A. Schäfer and A. V. Tarasov, *Phys. Rev.* **D62**, 054022 (2000).
- [35] K. Golec-Biernat and M. Wüsthoff, *Phys. Rev.* **D59**, 014017 (1999).
- [36] K. Golec-Biernat and M. Wüsthoff, *Phys. Rev.* **D60**, 114023 (1999).
- [37] S. Amendolia *et al.*, *Nucl. Phys.* **B277**, 186 (1986).
- [38] L.D. Landau and I.Ya. Pomeranchuk, *JETP***24**, 505 (1953).
- [39] A.B. Migdal, *Phys. Rev.* **103**, 1811 (1956).
- [40] L.V. Gribov, E.M. Levin and M.G. Ryskin, *Phys. Rep.* **100**, 1 (1983).
- [41] A.H. Mueller, *Eur. Phys. J.* **A1**, 19 (1998).
- [42] L. McLerran and R. Venugopalan, *Phys. Rev.* **D49**, 2233 (1994).